Cancer Immunology, Immunotherapy (2020) 69:1337–1352
https://doi.org/10.1007/s00262-020-02547-2

ORIGINAL ARTICLE

In vivo anti-MUC1$^+$ tumor activity and sequences of high-affinity anti-MUC1-SEA antibodies

Edward Pichinuk[1] · Michael Chalik[1] · Itai Benhar[2] · Ravit Ginat-Koton[2] · Ravit Ziv[2] · Nechama I. Smorodinsky[2] · Gabi Haran[3] · Christian Garbar[4] · Armand Bensussan[5] · Alan Meeker[6] · Thierry Guillaume[7,8] · Daniel B. Rubinstein[9] · Daniel H. Wreschner[2,9]

Received: 22 July 2019 / Accepted: 8 March 2020 / Published online: 26 March 2020

Abstract

Cleavage of the MUC1 glycoprotein yields two subunits, an extracellular alpha-subunit bound to a smaller transmembrane beta-subunit. Monoclonal antibodies (mAbs) directed against the MUC1 alpha–beta junction comprising the SEA domain, a stable cell-surface moiety, were generated. Sequencing of all seven anti-SEA domain mAbs showed that they clustered into four groups and sequences of all groups are presented here. mAb DMB5F3 with picomolar affinity for the MUC1 SEA target was selected for further evaluation. Immunohistochemical staining of a series of malignancies with DMB5F3 including lung, prostate, breast, colon, and pancreatic carcinomas revealed qualitative and qualitative differences between MUC1 expression on normal versus malignant cells: DMB5F3 strongly stained malignant cells in a near-circumferential pattern, whereas MUC1 in normal pancreatic and breast tissue showed only weak apical positivity of ductal/acinar cells. Humanized chimeric DMB5F3 linked to ZZ-PE38 (ZZ IgG-binding protein fused to Pseudomonas exotoxin) induced vigorous cytotoxicity of MUC1$^+$ malignant cells in vitro. The intensity of cell killing correlated with the level of MUC1 expression by the target cell, suggesting a MUC1 expression threshold for cell killing. MUC1$^+$ Colo357 pancreatic cancer cells xenotransplanted into nude and SCID mice models were treated with the chDMB5F3:ZZ-PE38 immunocomplex. In both transplant models, chDMB5F3:ZZ-PE38 exhibited significant in vivo anti-tumor activity, suppressing up to 90% of tumor volume in the SCID model compared with concomitant controls. The efficacy of chDMB5F3:ZZ-PE38 immunotoxin in mediating tumor killing both in vitro and in vivo strongly suggests a clinical role for anti-MUC1 SEA antibody in the treatment of MUC1-expressing malignancies.

Keywords MUC1 expression · Tumor antigens · Anti-MUC1 immunotherapy · Antibody–drug conjugation

Introduction

The MUC1 glycoprotein is overexpressed by a number of high-incidence, high-mortality human epithelial malignancies, including breast, prostate, pancreas, ovarian, and colon

Daniel B. Rubinstein and Daniel H. Wreschner have contributed equally to this work.

Electronic supplementary material The online version of this article (https://doi.org/10.1007/s00262-020-02547-2) contains supplementary material, which is available to authorized users.

✉ Daniel H. Wreschner
dwreschner@gmail.com

1 BLAVATNIK CENTER for Drug Discovery, Tel Aviv University, 69978 Ramat Aviv, Israel

2 School of Molecular Cell Biology and Biotechnology, Tel Aviv University, 69978 Ramat Aviv, Israel

3 Gynecology-Oncology Division, Mayanei Hayeshua Medical Center, Bnei Brak, Israel

4 Department of Biopathology, Centre Régional de Lutte Contre le Cancer, Institut Jean-Godinot, 51100 Reims, France

5 INSERM U976, Sorbonne Paris Cité, UMR-S 976, Université Paris Diderot, 75475 Paris, France

6 Department of Pathology, Johns Hopkins University School of Medicine, Baltimore, MD 21231, USA

7 Division of Hematology, Hôtel-Dieu, University Hospital Nantes, Nantes, France

8 Centre National de la Recherche Scientifique (CNRS), Université d'Angers, Université de Nantes, Nantes, France

9 BioModifying, LLC., Silver Spring, MD 20902, USA

carcinomas, by the malignant plasma cells of multiple myeloma, and on acute myelogenous leukemia [1–8]. Because of this preferentially high expression by malignant cells, MUC1 has been widely studied as both a target for directed cancer therapy and as a marker of disease progression [9]. The MUC1 transmembrane glycoprotein (MUC-TM) is a heterodimer consisting of an extracellular domain containing 20–125 repeats of a 20 amino acid-long sequence (the variable number tandem repeat, VNTR), a transmembrane domain, and a short cytoplasmic tail mediating intra-cellular signaling (Fig. 1, Panels I and IIa) [10–14]. MUC1 is auto-proteolytically cleaved within the SEA module, a highly conserved domain of 120 amino acids [12, 15]. This results in a large extracellular α subunit containing the tandem repeat array bound in a strong non-covalent interaction to a transmembrane β subunit containing the transmembrane and cytoplasmic domains of the molecule (Fig. 1, Panels I and IIa).

A number of anti-MUC1 antibodies have been reported in the literature with the majority directed against the highly immunogenic VNTR. Despite the ability of anti-VNTR antibodies to bind MUC1$^+$ cells in vitro, the shedding of the MUC1 α chain containing the VNTR into the peripheral circulation in vivo may compromise the efficacy of anti-VNTR antibodies. Once off the cell surface the MUC1 α chain, now freely circulating in the periphery, may bind and neutralize anti-VNTR or anti-VNTR-glycosylation antibodies tandem repeat antibodies, thereby limiting their ability to reach MUC1-expressing tumors.

Antibodies that recognize cancer-specific truncated O-glycoforms of the VNTR, such as antibodies PankoMab-Gex, 5E5, SM3, and VU-2-G7, may prove to overcome the potential toxicity of targeting MUC1 expressed by normal tissues. However, the limitations of targeting the α-chain VNTR, namely its shedding from the cell surface and its ability to bind circulating anti-MUC1 antibodies, remain [16–18].

Despite their therapeutic potential, no anti-MUC1 VNTR antibody has as yet been proven to be clinically effective [16, 19, 20]. Of note, Fiedler et al. [16] reported 16 cases of stable disease in a clinical trial of anti-VNTR cancer-specific glycosylation antibody PankoMab-Gex. The study was a PankoMab-Gex Phase I trial where the primary study objective was antibody safety, rather than anti-tumor efficacy, such that the cases of stable disease observed are difficult to interpret. Conclusions as to PankoMab-Gex's potential clinical efficacy must await a two-arm prospective study.

In contrast to the α chain and its VNTR, the MUC1 SEA domain formed by the interaction of the α-subunit with the extracellular portion of the β-subunit is a stable membrane-fixed molecular moiety (Fig. 1, Panel I). Previous studies described antibodies targeting the MUC1 SEA domain [21–23] as a therapeutic possibility, thereby avoiding antibody sequestration by the freely circulating shed α chain and circumventing a major impediment in the development of clinically effective anti-MUC1 antibodies.

The current study presents for the first time the sequences of seven monoclonal antibodies that recognize the MUC1 SEA domain. All such mAbs, designated the DMB series, specifically bind to cells expressing cell-surface MUC1 [22]. Analysis of these sequences showed that they clustered into four unique groups, namely [I] DMB5F3$^{[I]}$, [II] DMB7F3$^{[II]}$, [III] DMB4B4$^{[III\text{-}a]}$ and DMB10F10$^{[III\text{-}b]}$ and [IV] DMB4F4$^{[IV\text{-}a]}$, DMB10B7$^{[IV\text{-}b]}$, and DMB13D11$^{[IV\text{-}c]}$. DMB5F3 was chosen for further in-depth analyses as, of all DMB mAbs, it possessed a picomolar affinity, the highest affinity of all DMB mAbs.

Immunohistochemical staining of tissue microarrays with DMB5F3 of a series of malignancies showed quantitative differences in the density of MUC1 expression in tumor cells versus that in non-malignant cells. These were accompanied by qualitative differences in the architecture of MUC1 expression in malignancies at both the cellular and the tissue levels. The in vitro anti-tumor cytotoxic activity of a chimeric human DMB5F3 (chDMB5F3) immunocomplex was directly correlated with the level of MUC1 expression, showing that a threshold density of cell-surface MUC1 is necessary to elicit cytocidal activity. Furthermore, an in vivo human tumor xenograft model was established by injecting Colo357 human pancreatic cancer cells into nude and SCID mice and the xenotransplanted pancreatic tumor decreased profoundly following a series of intravenous (i.v.) administrations of the DMB5F3 immunocomplex. The results suggest that antibody DMB5F3-mediated immunotoxin targeting of the cell-surface MUC1 SEA domain may prove effective in the therapy of MUC1$^+$ malignancies, either alone or in conjunction with other therapeutic modalities.

Materials and methods

Reagents and antibodies

All reagents and chemicals were obtained from Sigma (St. Louis, MO), unless otherwise specified. Anti-MUC1 SEA module monoclonal antibody was generated as described [22]. Secondary antibodies used in cell counter-staining or in immunohistochemical development were obtained from Jackson ImmunoResearch Laboratories (Bar Harbor, ME).

Cell lines and cell cultures

DA3-PAR parental mouse mammary cells which do not express human MUC1, DA3-TM mouse mammary cells stably transfected with cDNA encoding for the full-length human MUC1-TM, cell lines T47D and ZR75 (human breast

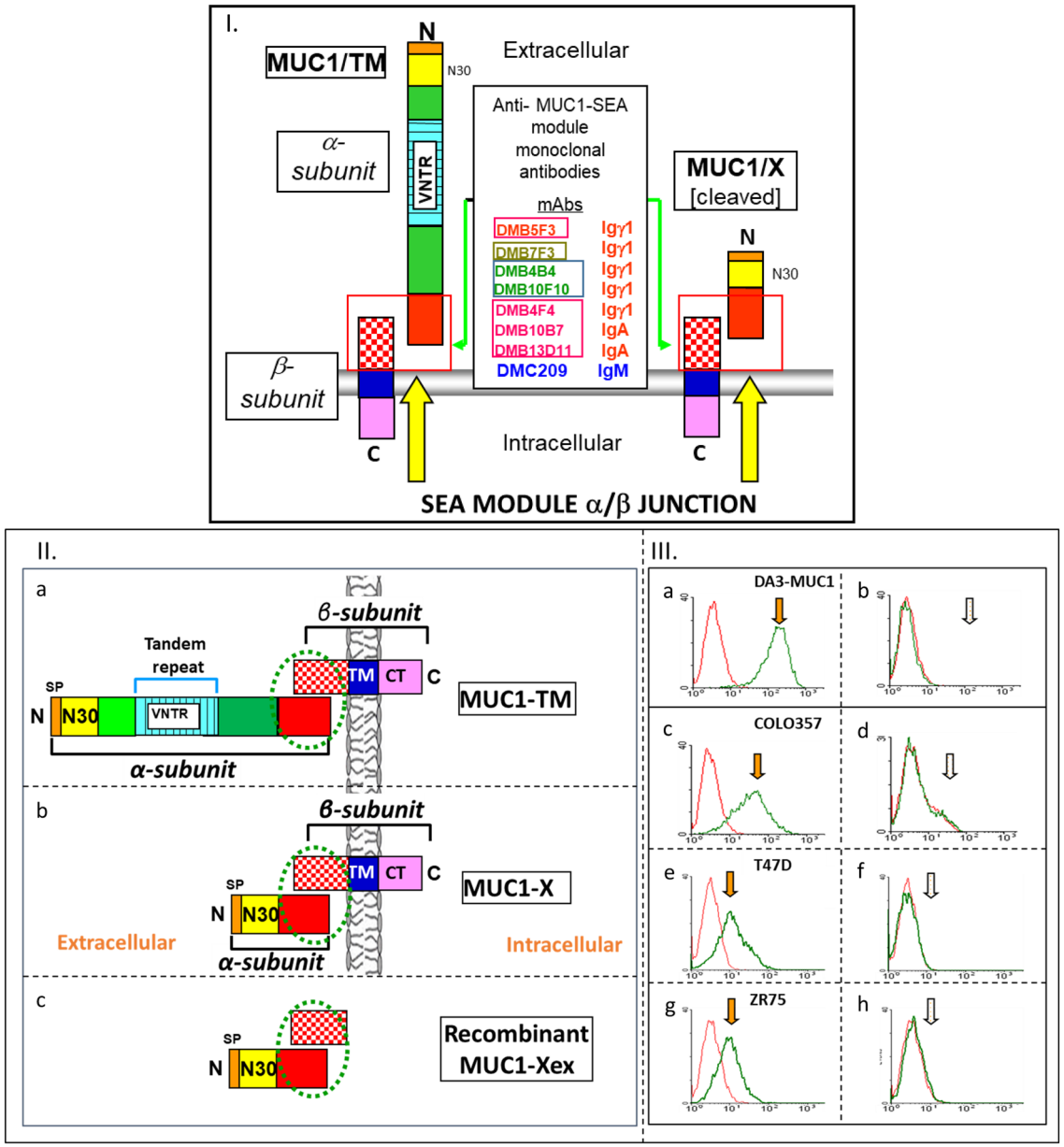

Fig. 1 Structure of MUC1 proteins, description of anti-MUC1-SEA module monoclonal antibodies, and flow cytometric analyses of the anti-MUC1 SEA antibody DMB5F3. **Panel I** The anti-MUC1-SEA module monoclonal antibodies, their immunoglobulin subtype, and groupings are indicated. **Panel II** The MUC1-TM, MUC1-X, and recombinant MUC1-X molecules schematically represented. (a) Going from the N (N) to the C terminus (C), MUC1-TM is composed of an N-terminal Signal Peptide (orange), followed by a 30 amino acid-long segment (N30, yellow), leading into sequences (green) that N-terminally and C-terminally flank the variable tandem repeat array (VNTR, blue). This is followed by a region (solid red) common to both the MUC1-X isoform (*b*) and to the soluble extracellular domain of MUC1 X, MUC1-Xex (*c*). The *β*-subunit extracellular domain consists of 58 amino acids (checkered red) immediately N-terminal to the transmembrane (TM, blue) and cytoplasmic (CT, magenta) domains. The SEA module comprises 120 amino acids, contributed by both the *α*- and *β*-subunits. Recombinant soluble MUC1-Xex protein (*c*) includes the signal peptide (light orange), the N-terminal 30 amino acid sequence (yellow) and the SEA module (solid and checkered red) regions. **Panel III** DA3 cells stably transfected with MUC1-TM (a, DA3-MUC1) or non-transfected DA3 cells (b), were reacted with anti-MUC1 SEA mAb DMB5F3, followed by an FITC-conjugate (green tracings). MUC1$^+$ human pancreatic cancer cell line Colo357 (*c*) and MUC1$^+$ breast cancer cells T47D and ZR75 (*e, g*) were reacted with DMB5F3 (green tracing). In all four panels, the red tracings represent cells bound to secondary antibody alone, and the green tracings (with orange arrows) that of cells reacted with both DMB5F3 and secondary antibody. MUC1 binding was entirely competed out by the presence of soluble MUC1-Xex protein (abrogated binding indicated by white arrows in *d, f* and *h*)

carcinomas), cell lines KB (human epidermoid carcinoma), Colo357 (human pancreatic carcinoma), N87 (human gastric carcinoma), and CHO-K1 (Chinese hamster ovary cells) were all grown in Dulbecco's Modified Eagle's Medium (DMEM), RPMI, and DMEM:F12 (1:1) culture media, as previously described [23].

Animals

Seven-week-old athymic (nude) and SCID mice (Harlan Laboratories, Madison, WI) were maintained until killing in facilities approved by the Tel Aviv University (TAU) Institutional Ethics Committee for Accreditation of Laboratory Animal Care, in accordance with the regulations and standards of the Israel Ministry of Health.

Flow cytometry analysis of DMB5F3 binding to MUC1-Expressing tumor cells

Following trypsinization, MUC1-expressing tumor cells were washed and incubated with DMB5F3 (0.5 µg/ml), with or without MUC1-Xex competitor (100 µg/ml), for 1 h at 4 °C. After washing with FACS buffer, fluorescein-labeled goat anti-mouse IgG was added for 45 min at 4 °C. Bound IgG was detected by flow cytometry on a FACSCalibur™ (Becton–Dickinson).

Immunohistochemical (IHC) staining with DMB5F3

Microarrays of normal and malignant pancreatic and breast tissue were purchased from US Biomax (Derwood, MD). Automated Immunological stains were obtained with the use of the Dako Autostainer Link 48 (Dako, Santa Clara, CA), according to the manufacturer's instructions. Antigenic retrieval was carried out with citrate buffer, for 30 min at room temperature. Endogenous peroxidase activity was blocked by the addition of Envision Flex Peroxidase Blocking Reagent (Dako) for 30 min, followed by incubation with DMB5F3 (5 µg/ml) for 2 h. The immunohistochemical reaction was detected by the addition of polymer dextran coupled with peroxidase and secondary antibodies for 15 min (EnVision-Flex/HRP, Dako) and diaminobenzidine for 10 min (DakoCytomation). This was followed by counterstaining with hematoxylin for 10 min.

Sequence determination of anti-MUC1-SEA module monoclonal antibodies

RNA was isolated from the DMB hybridoma series (see Fig. 1) with TRIzol® Reagent l, according to a technical manual for the reagent (Ambion Inc., Foster City, CA). The RNA sequence was determined as follows: cDNA was generated by reverse transcription of total RNA with the use of universal or isotype-specific anti-sense primers, according to the technical manual for PrimeScriptTM First Strand cDNA Synthesis Kit (Takara Bio Inc., Mountain View, CA). Amplification of VH and VL antibody fragments was carried out according to the standard operating procedure (GenScript, NJ, USA) which involves rapid amplification of cDNA ends, followed by separate cloning into a standard cloning vector. Clones with inserts of the correct sizes were sequenced by colony PCR and at least five colonies with such inserts were sequenced for each fragment, with the consensus sequence derived by alignment of the different clones.

Construction of chimeric chDMB5F3 for mammalian expression in Chinese hamster ovary cells

Human chimeric DMB5F3 (chDMB5F3) was generated from mouse DMB5F3. Briefly, the mammalian vectors pMAZ-IgH and pMAZ-IgL were used as backbones for expression of cDNA coding for the VH and VL regions of DMB5F3 fused to human γ1 heavy and human κ light chains, respectively [24]. The generated pMAZ IgH-chDMB5F3 and pMAZ IgL-chDMB5F3 vectors were used for transfection, and the resultant chimeric antibody chDMB5F3 was expressed in CHO cells. Stably transfected CHO cells secreted chDMB5F3, which was purified by protein-A affinity chromatography.

Preparation of the chDMB5F3: ZZ-PE38 immuncomplex

The generation of the chDMB5F3:ZZ-PE38 immunocomplex was carried out as described [22]. Briefly, chDMB5F3 was mixed with purified recombinant ZZ-PE38 protein in 20 mM Hepes buffer at a twofold molar excess of ZZ-PE38 and incubated for 2 h at 4 °C. Excess ZZ-PE38 and unconjugated chDMB5F3 antibody were removed by passage through a Sephadex G200 sizing column.

In vitro cell viability assay

T47D, KB, A431, and N87 cancer cells (20,000 cells/well) were seeded in 96-well cell culture plates and grown at 37 °C in 5% CO_2. After seeding, the chDMB5F3:ZZ-PE38 immunocomplex was applied directly to the cells at a concentration of 100 ng/ml. Negative controls consisted of target cells reacted with ZZ-PE38 toxin alone, unconjugated to chDMB5F3 antibody, or with chDMB5F3 monoclonal antibody alone, devoid of ZZ-PE38 toxin. Cell viability was assessed according to alkaline phosphatase activity/well. The results were calculated as the average of 2–3 experiments, performed in triplicate.

ELISA for determination of the binding of chDMB5F3:ZZ-PE38 immunocomplex to MUC1-Xex protein

To quantitate chDMB5F3 levels in mouse serum, ELISA immunoassay plates were coated with recombinant MUC1-Xex protein (see Fig. 1, Panel C1 for schematic structure), followed by blocking. At Days 1, 7, 15, and 28 after a single dose of 5 µg chDMB5F3:ZZ-PE38 immunocomplex, the mouse sera were applied to the ELISA wells at doubling dilutions and bound antibody was detected with horseradish peroxidase-conjugated goat anti-human Fc antibody. The results were calculated as the average of 2–3 experiments, performed in triplicate.

In vivo cytotoxicity assay

Two quantitatively measurable human tumor xenograft models were established, one in 7-week-old female athymic nude mice and one in 7-week-old SCID mice, by using Colo357, a MUC1$^+$ human pancreatic cancer cell line. A total 3×10^6 Colo357 cells suspended in a small volume (100 µl) of Hepes buffer were injected subcutaneously into the right flank of the mice. In both the nude and the SCID mouse studies, the mice were divided into three groups (5 mice/group): Group 1 received 5 µg chDMB5F3:ZZ-PE38 (0.25 mg/kg), Group 2 received 5 µg non-specific human Ig:ZZ-PE38 (0.25 mg/kg) and Group 3 received an equivalent volume of Hepes buffer alone. In the athymic nude mice (7-week-old female mice), administration of anti-MUC1 immunotoxin, non-specific immunotoxin or Hepes in the three experimental groups was initiated 24 h after the injection of Colo357 cells. The injection protocol consisted of a total six i.v. administrations on Days 1, 6, 9, 15, 22, and 29 in each experimental group (see black arrows along *x*-axis, Fig. 5). In the SCID mice (7-week-old female mice), chDMB5F3: ZZ-PE38, non-specific human Ig:ZZ-PE38, and Hepes were administered similarly, starting 24 h after injection of pancreatic tumor cells in each of the three groups. The overall protocol of administrations consisted of eight i.v. injections on Days 1, 4, 8, 11, 16, 24, 31, and 38 in each of the three groups. Tumor growth was assessed serially in each of the experimental groups with a digital caliper. Tumor volume was calculated according to the formula $0.5\times L\times W^2$, where L is tumor length, and W—tumor width [25]. All the animal experiments were approved by TAU's Institutional Review Board.

Statistics

Statistical analysis of in vivo tumor growth was performed according to a simple paired 1-tailed *t* test. A *p* value of less than 0.05 was considered statistically significant.

Results

Generation and sequencing of the DMB mAbs that bind the cell-bound MUC1 *α–β* junction and characterization of the DMB5F3 mAb

Anti-MUC1 monoclonal IgGs forming the DMB series were generated from hybridomas produced with spleen cells isolated from inoculated mice having high titers of polyclonal anti-MUC1-Xex antibody. The MUC1-Xex recombinant protein was used for immunization, and its relationship to the transmembrane MUC1-TM and MUC1-X proteins is shown in Fig. 1 (Panel II, compare c with b and a). A total of seven DMB mAbs were thus generated (Fig. 1, Panel I).

Sequencing of the resultant DMB mAbs showed that they clustered into 4 groups (Fig. 1, Panel I), denominated [I] DMB5F3$^{[I]}$, [II] DMB7F3$^{[II]}$, [III] DMB4B4$^{[III\text{-}a]}$ and DMB10F10 $^{[III\text{-}b]}$ and [IV] DMB4F4$^{[IV\text{-}a]}$, DMB10B7$^{[IV\text{-}b]}$, and DMB13D11$^{[IV\text{-}c]}$ (Fig. 2 for the amino acid sequences for each group and see Supplementary Figures 1a, 1b, 1c, and 1d for full nucleotide sequence, amino acid sequence, and genomic derivation of all groups). Sequences within each group revealed either unique mAb sequences as for DMB5F3$^{[I]}$ and DMB7F3$^{[II]}$ or mAbs with identical V_H and V_L sequences, as for Groups [III] and [IV] (Fig. 2 and Supplementary Figures 1a, 1b, 1c, and 1d).

The variable domains for all antibodies are typical of affinity maturation as expected from antibodies generated by prime-boost. All mAbs except for group [IV] mAbs DMB10B7$^{[IV\text{-}b]}$ and DMB13D11$^{[IV\text{-}c]}$ were Ig-γ1. Group [IV] contained three mAbs with identical V_H and V_L sequences- one (DMB4F4$^{[IV\text{-}a]}$) was of the Ig-γ1 subtype, whereas the remaining two (DMB10B7$^{[IV\text{-}b]}$ and DMB13D11$^{[IV\text{-}c]}$) were IgA.

All seven anti-MUC1 *α–β* junction mAbs robustly bound to cells expressing the transmembrane MUC1-TM protein, as assessed by flow cytometry ([22] and Fig. 1 Panel III). Representative mAbs from each of the four mAb groups were also assessed for their ability to detect MUC1-TM expression by immunohistochemistry performed on formaldehyde-fixed sections from Fresh Frozen (FF) tissues as well as on paraffin-embedded and formaldehyde-fixed (PEFF) tissues. Antibody DMB5F3$^{[I]}$-stained MUC1-expressing cells present in both FF and PEFF sections (see below), whereas the DMB7F3$^{[II]}$ and mAbs from group [IV] stained only on FF sections; in contrast, group [III] mAbs while binding well to MUC1-expressing cells as assessed by flow cytometry, were non-reactive with both FF and PEFF sections (data not shown).

The IgG1 monoclonal DMB5F3 demonstrated the highest binding affinity and, therefore, became the focus

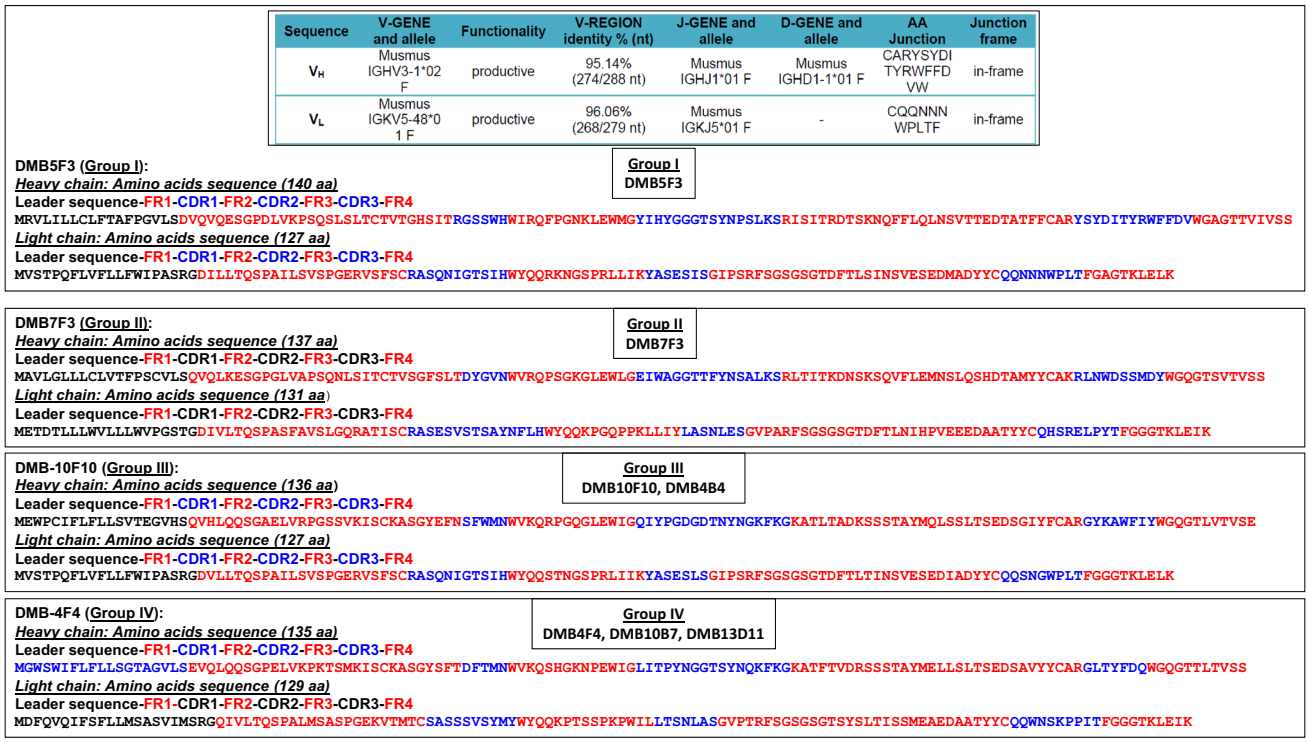

Fig. 2 Amino acid sequences of the variable domains of all anti-MUC1 SEA α–β junction DMB monoclonal antibodies. The nucleotide sequences of the variable regions of all anti-MUC1 SEA α–β junction DMB monoclonal antibodies was determined as described in Materials and Methods, and the deduced amino acid sequences of the 4 groups of mAbs are presented here. In addition, the genomic derivation of the Group I DMB5F3 mAb is shown at the top of the figure

of further study. The VH domain is derived from mouse germline V gene IGHV3-1*02 with 9 somatic mutations. It is 105/122(86%) identical to the highest scoring identical sequence in an NCBI BlastP search. The VL domain (V-kappa) is derived from mouse germline V gene IGKV5-48*01 with 3 somatic mutations (Fig. 2). It is 101/107(94%) identical to the highest scoring identical sequence in an NCBI BlastP search.

Flow cytometry analyses showed that DMB5F3 bound strongly to DA3 cells stably transfected with full-length MUC1 (DA3-TM) (Fig. 1, Panel III a), whereas non-transfected DA3-PAR cells, which do not express MUC1, were consistently negative (Fig. 1, Panel III b). Colo357, a MUC1- positive human pancreatic cancer cell line, as well as the MUC1 positive breast cancer cell lines T47D and ZR75, exhibited strong reactivity with DMB5F3 (Fig. 1, Panel III c, e and g). The addition of competing soluble recombinant MUC1-Xex protein (see Fig. 1, Panel II c, for the structure of recombinant MUC1-Xex), abolished all DMB5F3 cell binding (Fig. 1, Panel III, d, f and h), confirming antibody specificity.

IHC staining of human pancreatic and breast tissue sections with DMB5F3

To determine the degree to which monoclonal DMB5F3 binds to malignant and to normal tissues, a variety of malignancies in tissue microarrays, including breast, pancreatic, lung, prostate, and colon carcinomas underwent immunohistochemical staining (Fig. 3 and Supplementary Figures 2 and 3). The rationale to do extensive analyses for MUC1 expression, despite previous reports demonstrating MUC1 overexpression in malignancy lies in the significant fact that the anti-MUC1 mAbs described here recognize the MUC1 SEA module and were generated by immunization with recombinant MUC1-Xex protein (see Fig. 1, Panel II c), and not with the MUC1-TM protein (see Fig. 1, Panel II a), the form most commonly overexpressed by cancers. Analyses of MUC1 expression till now have been done with antibodies recognizing epitopes unique for the MUC1-TM protein, and particularly with anti-VNTR antibodies, and we thus wanted to see whether similar results pertain when using anti-MUC1-SEA domain antibodies. The tissue microarrays

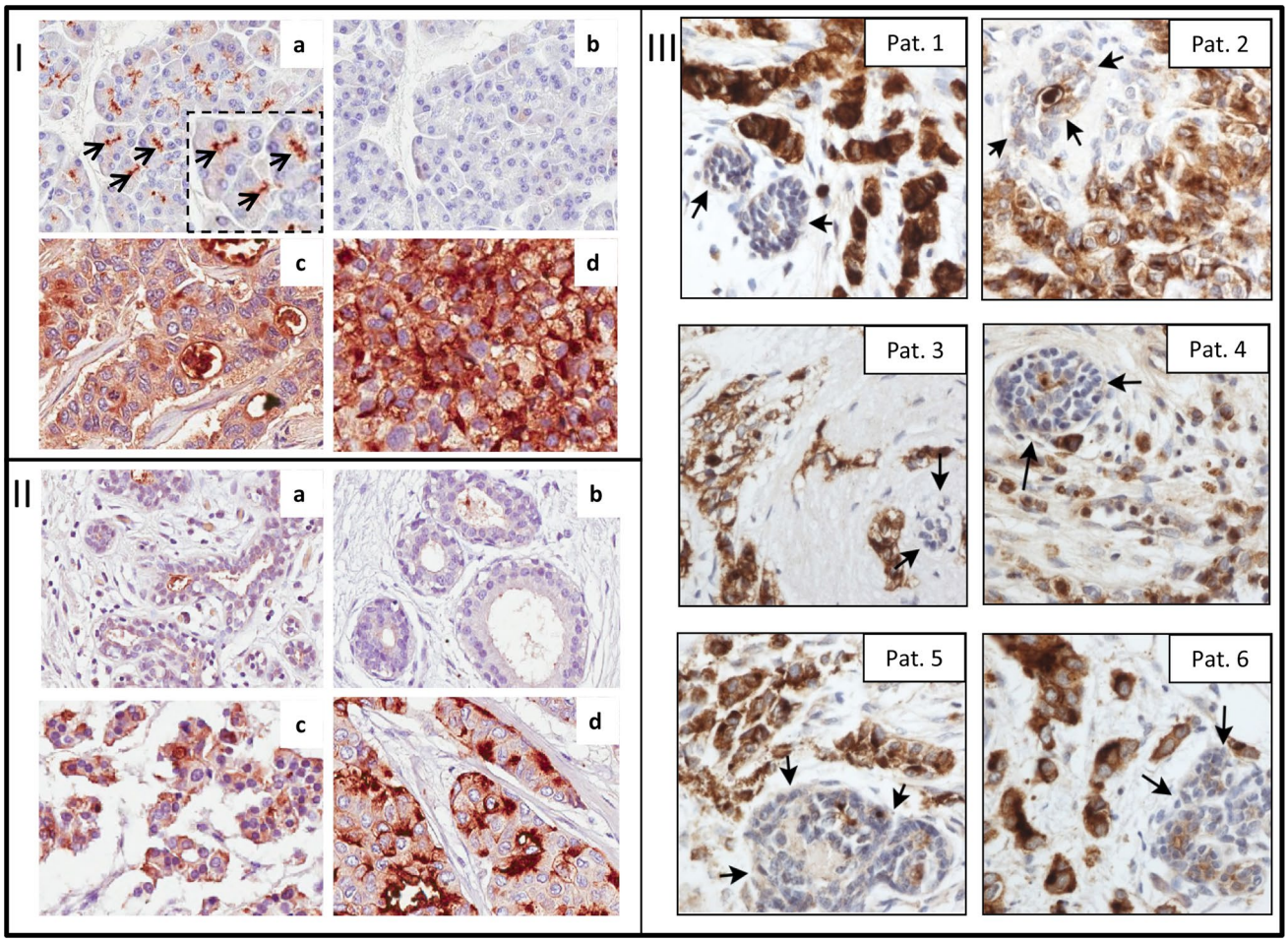

Fig. 3 Architecture of MUC1 expression delineated by anti-MUC1 SEA α–β junction DMB5F3. **Panel I** Paraffin-embedded microarrays of normal (images a and b) and malignant pancreatic tissue (images c and d) were stained with DMB5F3. DMB5F3 strongly stained malignant cells in a near-circumferential pattern (Panel I, images c and d), while in normal pancreatic acinar cells only weak apical positivity was seen (Panel Ia, black arrows). Addition of MUC1-Xex protein together with DMB5F3 abrogated staining (Panel Ib). **Panel II** Paraffin-embedded normal breast tissues (images a and b) and malignant invasive ductal breast adenocarcinomas (images c and d) from 4 patients were stained with DMB5F3 antibody. **Panel III** Breast carcinoma biopsy specimens, each consisting of tumor surrounded by adjacent non-malignant tissue, stained with DMB5F3 (images Pat. 1 to Pat. 6). The presence of both malignant and non-malignant tissue assured that differences in staining patterns were not due to differences in technique. In each DMB5F3 strongly stained invasive cancer epithelial cells in a near-circumferential pattern (brown staining). In contrast, adjacent normal glandular epithelial cells showed only weak apical positivity (black arrows)

used for these analyses included the following (Biomax microarray designation in parenthesis): 6 pancreatic tumors with adjacent non-neoplastic tissues (PA241); 40 different pancreatic tumors and 8 normal pancreatic tissues (PA483); 3 samples each of breast plasma cell mastitis, adenosis and fibroadenoma and 36 invasive breast ductal carcinomas plus 2 invasive breast lobular carcinomas (BR963a) and 10 cases each of colon, breast, prostate, lung, and colon carcinoma, in addition to two sections each from the corresponding normal tissues (TP481). A representative composite array of normal and malignant tissues immunohistochemically stained with DMB5F3 is shown in Fig. 3. Of the 46 pancreatic tumors (in microarrays PA241 and PA483), 44 exhibited strong reactivity with DMB5F3; tumor cells stained in a near-circumferential pattern (for examples see Fig. 3, Panel I, c and d). In contrast, normal pancreatic tissue DMB5F3 reactivity was restricted to the luminal surface of the ductal pancreatic epithelial cells (Fig. 3, Panel I, a).

Of the breast tissue samples analyzed on the BR963a microarray (Supplementary Figure 2), minimal to no staining was seen in non-malignant tissues that included normal breast tissue, plasma cell mastitis, adenosis, and fibroadenoma. This was in contrast to the 36 invasive breast ductal carcinomas, 21 of which showed very high DMB5F3 reactivity, 4 showed low levels of expression, and 11 samples showed little to no expression (for examples,

see Supplementary Figure 2). In addition to the limited expression in breast and pancreatic ducts (see above), high MUC1 expression as assessed by immunohistochemistry with DMB5F3 was observed in epithelial cells forming the lumens of the kidney distal tubular structures (see Fig. 7 in [26]). Here, as in normal breast and pancreatic tissues, MUC1 expression had an additional characteristic: It was restricted solely to the apical surface of the distal tubular cells forming the ductal lumens, a location, of very limited access to antibodies present in the peripheral circulation. The examined pancreatic tissues included both acinar (Fig. 3, I-d) and ductal adenocarcinomas (Fig. 3, I-c and Supplementary Figure 3, Panel II, b, c), whereas malignant breast tissues in the microarray consisted of invasive ductal carcinomas (Fig. 3, II-c, II-d). Malignant cells from pancreatic carcinomas (Fig. 3 Panel I-c and I-d and Supplementary Figure 3, Panel II, b, c), breast carcinomas (Fig. 3 Panels II-c and II-d, Panel III, patients 1–6, and Supplementary Figure 2), and lung, prostate and colon carcinomas (Supplementary Figure 3, Panel I, a, b and c, respectively, insets a, b' and c' at higher magnifications) were strongly reactive with DMB5F3, with near-circumferential cellular staining. In contrast, normal pancreatic acinar cells showed only weak apical positivity (indicated by black arrows in Fig. 3, Panel I, a-inset at higher magnification, and Supplementary Figure 3, Panel II, a), consistent with a previous description [27]. Normal breast ductal epithelial cells (Fig. 3, Panels II-a and II-b, and Supplementary Figure 2) and normal gland-like structures formed by non-malignant epithelial cells adjacent to the malignancy on the microarray exhibited weak apical positivity (Fig. 3, Panel III, presents biopsy sections from six patients [Pat.1–Pat.6]; normal gland-like structures indicated by black arrows). This was in marked contrast to malignant cells in the same section that stained strongly with DMB5F3 anti-MUC1-SEA antibody (Fig. 3, Panel III). As malignant and non-malignant material were on the same microarray sample and, therefore, simultaneously and uniformly stained, the possibility that mere technical differences in handling and staining could account for the findings may be excluded. Moreover, the finding that soluble MUC1-Xex (see Fig. 1) out competed cell staining confirmed the anti-MUC1 specificity of DMB5F3 (compare Fig. 3, Panels I-a and Panel I-b, respectively).

To extend these observations to other tumor types, lung, prostate, and colon carcinomas were examined immunohistochemically with DMB5F3 (Supplementary Figure 3, Panel I, a, b, and c). The results showed a pattern of MUC1 distribution similar to that observed in the breast and pancreatic carcinomas (Fig. 3). In addition to the increased density of MUC1 expression at the cellular level, distinctions in MUC1 architecture were observed again: Anti-MUC1-SEA DMB5F3 bound malignant cells in a near-circumferential pattern. Here too, staining with DMB5F3 was abolished in the presence of competing soluble MUC1-Xex protein, attesting to the specificity of DMB5F3 (data not shown) and no staining was observed with non-immune mouse immunoglobulin (compare Supplementary Figure 3, Panel I, a, b, c, and d with a", b", c", and d"). The majority of the nearly 50 lung, prostate, colon, breast, and pancreatic adenocarcinoma tissues examined in the microarrays showed a similar IHC staining pattern, a minority expressing lower amounts of MUC1 and a few with negligible MUC1 expression. This non-uniformity is consistent with the heterogeneity of tumor phenotypes in general and of MUC1 in particular [1, 6]. Because pancreatic carcinoma, a high-mortality MUC1-expressing malignancy, was selected for the in vivo studies (see below), pancreatic tumor tissue from an additional series of patients was examined to confirm the altered tumor-associated architecture of MUC1 expression (see representative staining in Supplementary Figure 3, Panel II, b and c). Although these analyses reveal increased circumferential DMB5F3 immunoreactivity over the entire cell surface of the adenocarcinoma cancer cells, the following two caveats are pertinent: (a) immunohistological analyses are only semi-quantitative and (b) in some cases MUC1 is strongly expressed within the cell, rendering comparisons of surface expression difficult. Notwithstanding these two provisos it is clear that cancer cells derived from adenocarcinomas exhibit high cell-surface immunoreactivity with DMB5F3.

In vitro cytotoxicity of the chDMB5F3: ZZ-PE38 immunocomplex

After demonstrating the reactivity of DMB5F3 with cancer cells expressing cell-surface MUC1 both in cell lines (Fig. 1, Panel III) and in microarrays of tissue biopsies (Fig. 3 and Supplementary Figures 2 and 3), the antibody's ability to ferry a cytotoxic moiety into malignant cells was examined. The ZZ-PE38 fusion protein consists of Pseudomonas exotoxin PE38 and the IgG-binding ZZ-domain derived from Protein A. Because the ZZ domain binds tightly to human Fc and shows negligible binding to mouse IgG1 Fc, and with the DMB5F3 sequence in hand (Fig. 2), a chimeric DMB5F3, designated chDMB5F3 was generated by substituting the mouse IgG1-Fc portion of the antibody with human Fc. ZZ-PE38 was then added to the chimeric (ch) DM5F3 to form the immunotoxin complex, as described in Materials and Methods.

As the ZZ-PE38 toxin alone is unable to bind to or internalize into cells, all tumor cytotoxicity induced by the DMB5F3-ZZ-P38- immunocomplex is due solely to cell binding and internalization by the anti-MUC1 DMB5F3 immunocomplex [24]. MUC1$^+$ T47D cells (breast carcinoma) and KB cells (epidermoid tumors) (were found to be sensitive to chDMB5F3:ZZ-PE38 immunocomplex-mediated inhibition of cell growth, with tumor cytotoxicity seen

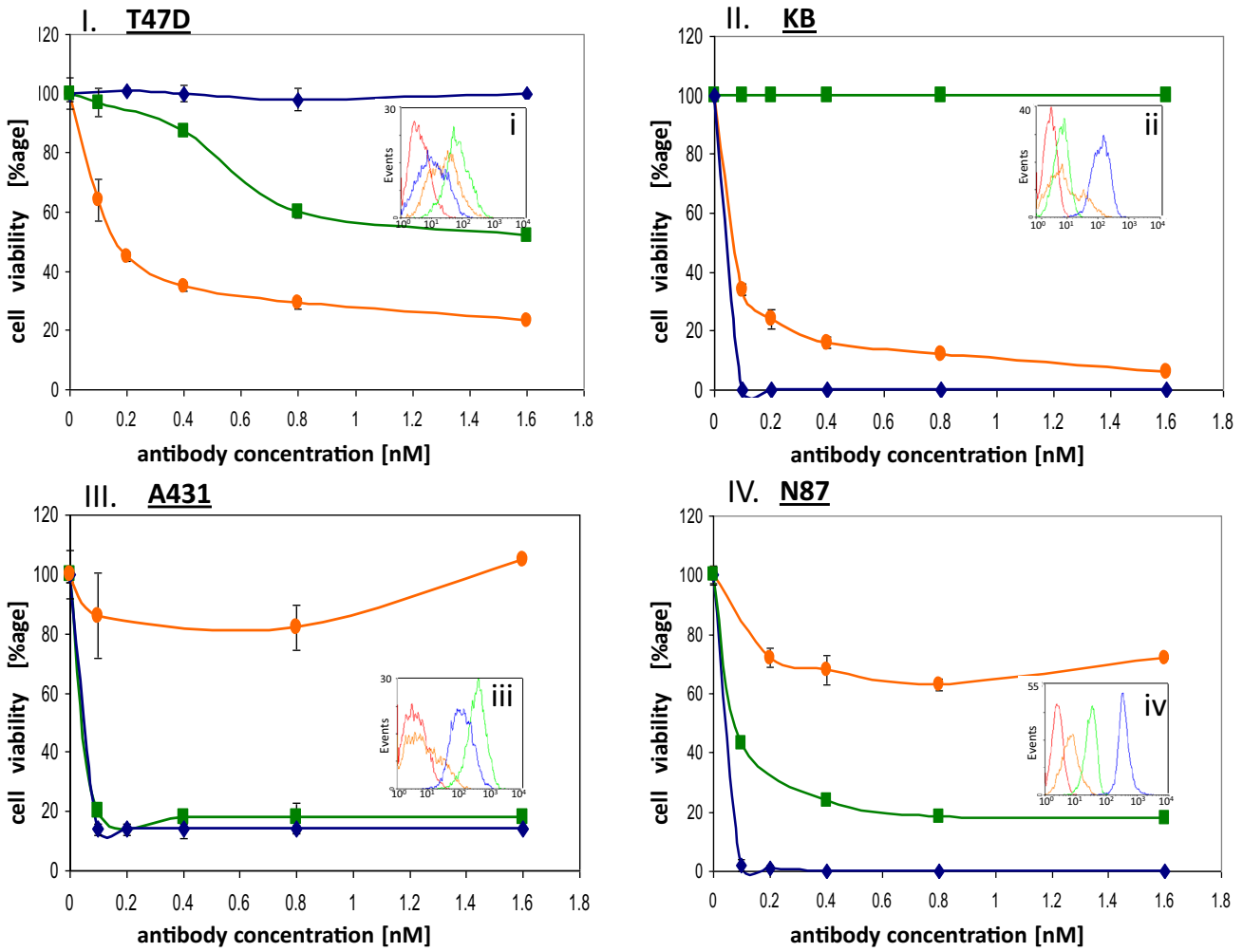

Fig. 4 Comparative cytocidal activity of chDMB5F3, Erbitux, and Herceptin: ZZ-PE38 immunotoxins on human tumor cells. Tumor cell lines T47D, KB, A431, and N87 (Panels I–IV, respectively), were treated with immunotoxin chDMB5F3:ZZ-PE38 (orange tracing), Erbitux:ZZ-PE38 (blue tracing), and Herceptin:ZZ-PE38 (green tracing) at varying antibody concentrations (*x*-axis). Cell viability was assessed with the alkaline phosphatase assay (*y*-axis). Total (100%) viability was determined in control wells to which ZZ-PE38 toxin (5 nM) alone had been added. Each cell line was cytometrically analyzed (see insets i–iv) with chDMB5F3 (orange), Erbitux (blue) and Herceptin (green) at concentrations of 300 ng/ml. Background fluorescence is represented by red tracings

at antibody concentrations as low as 200 pM (Fig. 4, Panels I and II, see insets i and ii for their MUC1 expression shown by the orange tracing). Soluble MUC1-Xex protein in concentrations as low as 500 nanograms/ml directly competed with chDMB5F3:ZZ-PE38, resulting in a marked reduction in cell killing, as shown for T47D cells (see Fig. 4 in [23]) and for Colo357 pancreatic cancer cells and ZR75 breast cancer cells (see Fig. 7 in [22]). This confirmed the specificity of DMB5F3 binding to MUC1 and was consistent with the complete abolition of DMB5F3 binding by MUC1-Xex seen in the flow cytometry (Fig. 1, Panel III, d, f and h). In contrast, T47D breast cancer cells expressing low, yet clearly detectable, levels of EGFR1 (Fig. 4, Panel I, inset i) were insensitive to Erbitux®:ZZ-PE38 (Fig. 4, Panel I, blue tracing), and only partially sensitive to Herceptin®:ZZ-PE38 (Fig. 4, Panel I, green tracing). KB cells, which expressed low, yet clearly detectable levels of erbB2-EGFR2 (Fig. 4, Panel II, inset ii, green tracing), were insensitive to Herceptin®:ZZ-PE38 (Fig. 4, Panel II, green tracing). Cells expressing markedly lower levels of MUC1 such as N87 showed approximately 40% cytotoxicity, contrasting with the high MUC1 expression and high cytotoxicity seen in T47D and KB cells (compare Fig. 4, Panel IV, inset iv with Panels I and II, and their respective insets, i and ii). A431, the lowest MUC1 expresser of all cell lines investigated, contained a major population of cells that showed no MUC1 expression (Fig. 4, inset iii) with only a much smaller subpopulation expressing low-level MUC1 (compare Fig. 4, inset iii with insets i, ii and iv). Consistent with this low level of MUC1 expression, chDMB5F3:ZZ-PE38 immunocomplex

resulted in very little limited cytotoxicity of A431. These results indicate that a threshold level of cell-surface MUC1 expression and density is a necessary requirement to elicit cytotoxicity. A similar phenomenon is observed with the absence of cytotoxicity of Herceptin-immunotoxin-complex when applied to KB cells despite low, yet detectable, levels of erbB2-EGFR2 expression by these cells (Fig. 4, Panel II), and Erbitux-immunotoxin-complex when applied to T47D cells that also express low, yet detectable, levels of EGFR1 (Fig. 4, Panel I).

Despite this evidence for a threshold, the exact number of cell-surface MUC1 molecules required for chDMB5F3:ZZ-PE38-mediated cytotoxicity remains, as yet, unknown.

Pharmacokinetics of chDMB5F3 in nude mice

In order to be an effective therapeutic agent, circulating anti-MUC1-SEA DMB5F3 must remain biologically active for a threshold period of time. The in vivo stability of chDMB5F3 was therefore evaluated by assessing serum levels on Days 1, 7, 14, and 28 following i.v. administration. The results showed that compared with Day 7, serum levels of antibody chDMB5F3 on Days 14 and 28 were twofold and fourfold decreased, respectively (Fig. 5, Panel b), consistent with previously reported half-lives in mice of in vitro generated chimeric IgGs and of antibodies in clinical use [28]. As for the toxin conjugate, the half-life of Pseudomonas exotoxin has been shown to be extended by linkage to IgG [29].

In vivo cytotoxicity of chDMB5F3:ZZ-PE38 immunocomplex in xeno-transplanted human tumors

Administration of the chDMB5F3:ZZPE38 immunocomplex to nude mice xenotransplanted with MUC1$^+$ human pancreatic Colo357 cells resulted in a marked cytocidal effect with a reduction in tumor volume at Days 21, 28, and 35 versus that in the control groups, which had received Hepes buffer or matched isotype IgG-ZZ: PE38 (Fig. 5, Panel a). Upon completion of chDMB5F3:ZZPE38 immunocomplex administration, the tumor volume of the treated group

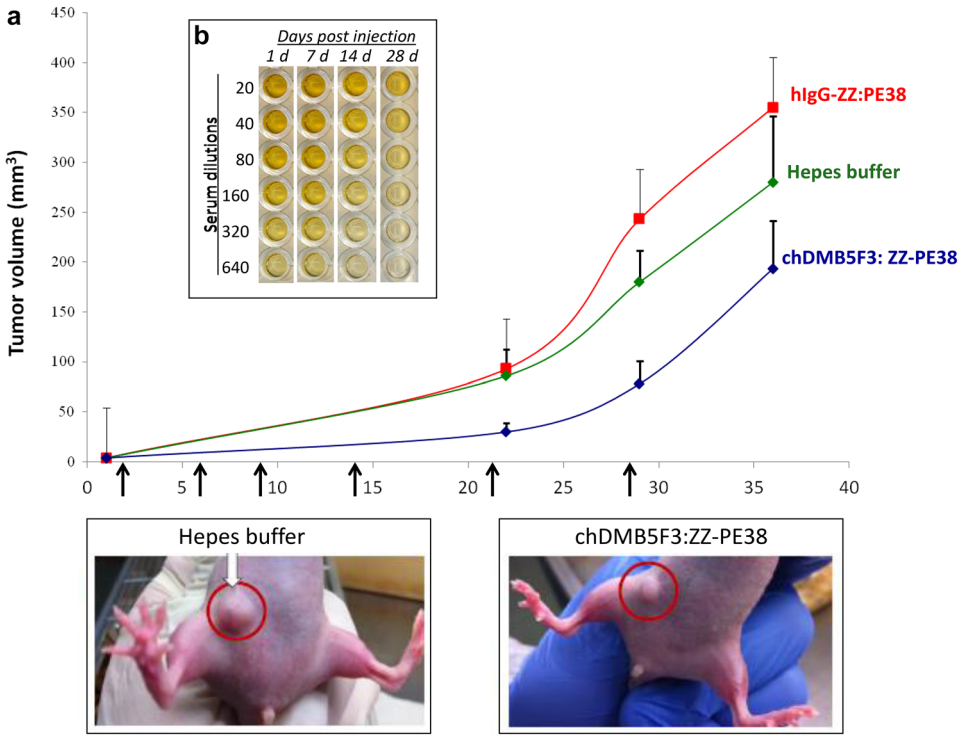

Fig. 5 In vivo cytotoxicity of chDMB5F3:ZZ-PE38 in human pancreatic tumor xenotransplanted into nude mice **Panel a** Nude mice were inoculated with MUC1$^+$ pancreatic tumor Colo357 (Day 0). At 24 h, and on Days 1, 6, 9, 14, 22, and 29 chDMB5F3: ZZ-PE38, matched isotype IgG-ZZ: PE38 (5 µg per injection) or Hepes buffer were injected i.v. (time points indicated by arrows). Tumor volume was measured weekly during the injection period to Day 38 (see "Materials and methods" section) in mice receiving chDMB5F3: ZZ-PE38 (blue curve), isotype hIgG-ZZ: PE38 (red curve), and Hepes buffer (green curve). Tumor volume in mm^3 appears on the *y*-axis. Photo images depict the tumors in the Hepes control mice (left image) and in mice receiving chDMB5F3: ZZ-PE38 (right image). **Panel b** To quantitate serum half-life of the anti-MUC SEA DMB5F3-ZZ-P38 immunotoxin, a single 5 µg dose was administered to mice, and serum levels measured by serially diluted Elisas. Compared with Day 7 (7 days), serum levels of chDMB5F3 on Days 14 (14 days) and 28 (28 days) were twofold and fourfold decreased, respectively

increased progressively in direct parallel with that in the control groups and by Day 40 (when the animals were sacrificed) the tumor volume in all three groups reached the 200–400 mm^3 range (Fig. 5 Panel a).

A factor conceivably limiting the cytotoxic efficacy of the chDMB5F3:ZZPE38 immunocomplex in xenotransplanted nude mice is endogenous circulating antibody, which by interacting with the ZZ linker may at least partially displace ZZ-PE38 toxin from chDMB5F3. Although ZZ does not bind mouse IgG1, it can bind mouse IgG2. Limitation in immunotoxin efficacy by displacement does not reflect defective binding of antibody chDMB5F3 to tumor cell-surface MUC1, but arises from toxin loss owing to reduced ZZ-mediated linkage of ZZ-PE38 to the chDMB5F3 antibody. To avoid this complicating factor, a nearly identical study in SCID mice, which lack detectable endogenous antibody, was then performed. As in the nude mouse protocol, transplanted SCID mice were divided into three groups, one receiving the chDMB5F3:ZZPE38 immunocomplex, one receiving a matched isotype IgG-ZZ:PE38, and one receiving Hepes buffer alone, each initiated 24 h after injection of pancreatic tumor. As noted in Methods, the protocol consisted of serial administrations in each group on Days 1, 4, 8, 11, 16, 24, 31, and 38. The chDMB5F3:ZZ-PE38 immunocomplex exhibited a marked anti-tumor effect: In SCID mice treated with chDMB5F3:ZZ-PE38, the volume

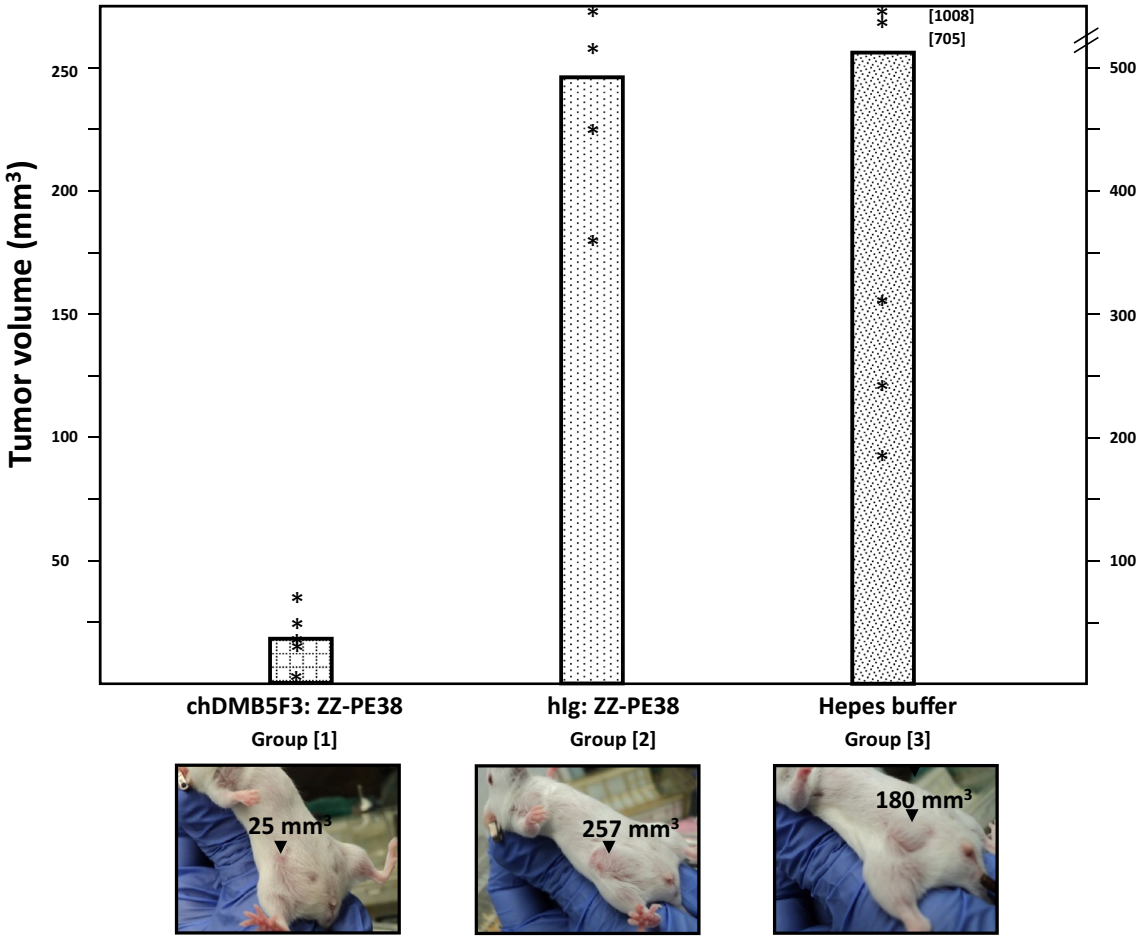

Fig. 6 chDMB5F3:ZZ-PE38 immunotoxin cytotoxicity in vivo: Ablation of $MUC1^+$ pancreatic cancer xenograft in SCID mice. SCID mice were inoculated subcutaneously with Human Colo357 pancreatic cancer cells on Day 0, and divided into three groups: Group [1] received 5 µg of chDMB5F3:ZZ-PE38, Group [2] received 5 µg of non-specific human Ig:ZZ-PE38 conjugate, and Group [3] Hepes buffer on Days 1, 4, 8, 11, 16, 24, 31, and 38. Tumor volumes were compared 49 days following cell inoculation (see Methods). The histograms represent the average tumor volumes for each group, each asterisk represents the value for an individual mouse. The *y*-axis to the left represents tumor volume (in mm^3) for Groups 1 and 2; the *y*-axis to the right represents tumor volumes in Group 3 (Hepes buffer) extended to 500 mm^3 to include the larger tumors in the control group. Two points in Group 3 with values above the 500 mm^3 point represent tumor volumes of 705 mm^3 and 1008 mm^3. Below the histograms, representative mice from each group are pictured together with their tumor volumes at the conclusion of the 49-day tumor measurement period. Pictured are mice which received chDMB5F3:ZZ-PE38 (left image), which received non-specific human Ig:ZZ-PE38 conjugate (middle image), and which received Hepes buffer (right image)

of xenotransplanted Colo357 human tumors was reduced by as much as 90% versus that in the control groups (Fig. 6). The actual values (in mm^3) for tumor volumes are as follows: Group [1] mice treated with the chDMB5F3-immunotoxin 2, 14, 16, 25, and 36 mm^3; Group [2] mice treated with the hIgG (non-specific-immunotoxin) 180, 225, 258, and 270 mm^3 (lack of tumor take for one mouse in this series is not included); and Group [3] mice treated with Hepes buffer 180, 245, 304, 705, and 1008. The extended scheduling of chDMB5F3: ZZ-PE38 administration to Days 31 and 38 assured an anti-tumor effect as late as Day 49.

Discussion

The sequences of anti-MUC1-SEA module DMB mAbs all of which bind to cell-surface MUC1 are presented here. These data show that the seven DMB mAbs segregate into 4 unique groups. Groups [I] and [II] each comprise one solitary mAb, whereas groups [III] and group [IV] contain 2 and 3 mAbs, respectively. We have previously shown (see Fig. 5 in [22]) that the group [I] DMB5F3 antibody possesses a very high binding affinity and because of its picomolar affinity, in the present study we have focused on this mAb. Using the sequence of DMB5F3, a recombinant DMB5F3 immunotoxin complex was generated. It showed marked cytocidal activity both against $MUC1^+$ tumor cells in vitro and most significantly, in an in vivo human pancreatic tumor xenotransplant model system.

Because of its overexpression on a variety of high-incidence malignancies, MUC1 has been long identified as a very promising immunotherapeutic target. However, almost all anti-MUC1 antibodies developed to date for therapeutic targeting of MUC1 are directed against the highly immunogenic polymorphic array of 20–125 tandem repeats in the MUC1 α-chain (the VNTR; Fig. 1, Panels I and IIa). Although useful in immunohistochemical detection of MUC1 on the cell surface, antibodies directed against the α-chain VNTR have not proven to be therapeutically beneficial against MUC^+ malignancies likely because the α-chain is only intermittently bound to the cell in vivo.

As discussed in the Introduction section, cancer-associated aberrant glycosylations of the MUC1 VNTR may prove to have distinct advantages as antibody tumor targets, together with the inherent potential disadvantages common to all targets on the shed MUC1 α chain [16, 17, 30].

Although targeting membrane-bound MUC1 via the β-subunit might seem to provide a possible solution (see Fig. 1 Panel I), the β-subunit alone failed to elicit a significant humoral response (data not shown) precluding its use for hybridoma formation. In line with this, we were unable to generate anti-β chain antibodies capable of stably binding to MUC1-expressing cells [21, 22]. Recently, generation of a solitary anti-MUC1 monoclonal antibody derived from mice immunized with the β-subunit has been reported [31]. This stands in contrast to the four independent groups of mAbs described here that target the MUC1 α/β junction. Rather than targeting the β-subunit alone, the stable structure formed by interaction of both the α and the β MUC1 subunits provides a suitable, and possibly an ideal, construct for targeting membrane-bound MUC1 [12, 15]. The membrane-bound SEA module comprising the C-terminal part of the MUC1 α-subunit bound to the extracellular portion of the membrane-bound β-subunit provides just such a stable structure (see Fig. 1, Panels I and II for schematic representation).

Whereas the MUC1-X isoform contains the same intracellular and membrane domains as the full MUC1-TM molecule (Fig. 1, Panels I and II), its extracellular domain is composed solely of the 120 amino acid-long SEA module fused to a 30N-terminal amino acid domain of MUC1 (Fig. 1, Panels I and II b). In the present study, robust reactivity of the anti-MUC1-SEA module DMB5F3 was initially confirmed by flow cytometry with a variety of $MUC1^+$ tumor cell lines including Colo357, T47D and ZR75, (Fig. 1, Panel III, c, e, and g). The results clearly show the ability of DMB5F3 to bind native MUC1-TM expressed on malignant cell lines. The specific reactivity of DMB5F3 with MUC1 on malignant cells in tumor-derived tissue was confirmed by immunohistochemical staining of fixed tissue arrays of human lung, breast, prostate, colon, and pancreatic carcinomas (Fig. 3 and Supplementary Figures 2 and 3).

Ideally, for clinical use as therapeutic targets tumor-associated antigens should be expressed solely by malignant cells and not by their normal cell counterparts. However, almost all documented 'tumor-target' proteins, including those with proved clinical therapeutic use, are expressed at constitutive levels by normal cells and up-regulated in malignancy. Such is the case for EGFR1, HER2, VEGFR, CD20, CD33, and such is the case for MUC1 [32, 33]. However, there are two determinant factors underlying the preferential therapeutic potential of anti-MUC1 antibodies: (1) The quantitative density of MUC1 expression is markedly greater on tumor than on normal cells, and (2) the qualitative distribution and architecture of MUC1 on malignant cells differs from that of normal cells.

Quantitative differences in MUC1 expression between tumor and normal cells have been previously reported [34]. The present study extends and better defines cancer-related MUC1 expression: As shown (Fig. 3 and Supplementary Fig. 3, Panel IIa), MUC1 expression in normal secretory tissue was limited to the apical surface of secretory epithelial cells in the direction of the ductal lumen. As a result, administered anti-MUC1 antibody will not have direct, unimpeded access to MUC1 expressed on the surface of such non-malignant cells. In contrast, tumors lose their normal architecture

both at the tissue and cellular level, so that MUC1 expression is no longer limited to the relatively inaccessible apical surface. Rather, MUC1 is expressed circumferentially over the entire cell surface of the malignant cells (Fig. 3, Supplementary Figures 2 and 3). This loss of normal architecture renders the MUC1 expressed by tumor cells more accessible to administer anti-MUC1 antibodies. In addition to these qualitative differences in MUC1 architecture, the quantitative density of cell-surface MUC1 expression is elevated in $MUC1^+$ malignancies versus that in normal, non-malignant cells (Fig. 3 and Supplementary Figures 2 and 3) [2, 4, 35]. This quantitative difference can be exploited therapeutically.

In order to facilitate investigation into their therapeutic potential, all anti-[MUC1-SEA module] DMB mAbs were sequenced, and in the present study, the DMB5F3 sequence (Fig. 2) was used to generate 5F3 antibodies possessing Fc portions other than those of mouse IgG1. Furthermore, elaboration of the DMB5F3 sequence should allow generation of high-affinity anti-MUC1-SEA module mAbs to effectively target $MUC1^+$ tumors.

The cytotoxicity of the chDMB5F3: ZZ-PE38 immunocomplex directly correlated with the level of MUC1 expression and in order to elicit cytocidal activity at the dose range used, the immunocomplex required a threshold expression level of cell-surface MUC1 (Fig. 4). Tumor-expressing MUC1 above this threshold level will be affected, whereas normal cells expressing lower constitutive levels of MUC1 will not, thereby providing a therapeutic safety window for minimizing antibody-induced toxicity [36]. Furthermore, the anti-MUC1 SEA antibody DMB5F3 binds to $MUC1^+$ cells with a high picomolar affinity. Thus, only a limited amount of such high-affinity antibody would be needed for an in vivo effect, and MUC1 overexpressed by tumors and architecturally exposed on the tumor cell surface (Fig. 3 and Supplementary Figures 2 and 3) would tend to be bound therapeutically by most or nearly all of the administered anti-MUC1 SEA antibody drug conjugate (ADC).

In the SCID mouse model, pancreatic tumor volume in mice treated with the chDMB5F3:ZZ-PE38 immunocomplex was reduced by up to 90% versus that in the controls (Fig. 6). The design of the study entailed injection of the immunocomplex at the time of, or immediately following xenotransplantation of human tumor, allowing to correlate tumor cell burden (number of tumor cells injected) with administered immunocomplex. This experimental design was specifically chosen to provide a proof-of-principle demonstration of the in vivo anti-tumor activity of the immunocomplex, rather than direct mimicking of clinical administration where immunotoxin is administered for preexisting tumors. Furthermore, the experimental protocol was not designed as a dose–response study.

The mouse xenotransplant model used here cannot directly address the issue of anti-MUC1 ADC binding to $MUC1^+$ non-malignant cells and its possible attendant toxicity as chimeric anti-MUC1 SEA antibody chDMB5F3 binds only human, and not murine MUC1. An ideal system in which to address this issue is the transgenic mouse that expresses human MUC1 [37]. Significantly, however, we have here clearly demonstrated proof-of-concept that a circulating anti-MUC1-SEA module DMB5F3 mAb bound to toxin can in vivo target, internalize and kill a MUC1-expressing human tumor. In contrast to the SCID mice that are devoid of immunoglobulins, immunocompetent human MUC1 transgenic mice have high levels of circulating endogenous immunoglobulins. The immunotoxin complex in the present study consists of the ZZ-PE38 toxin bound in a *non-covalent* manner to the hFc part of the chimeric chDMB5F3 mAb via the ZZ portion (the Ig binding domain of Protein A) of the ZZ-PE38 fusion protein. Because of the non-covalent nature of toxin bound to DMB5F3, circulating endogenous mouse immunoglobulins present in human MUC1 transgenic mice, and especially those with high affinity for the ZZ-domain, such as mouse Ig-gamma2, can displace chDMB5F3 and bind to ZZ-PE38, thereby rendering the toxin-targeting function of DMB5F3 relatively ineffective. In order to assess off-target toxicity in the human MUC1 transgenic mouse model, the toxin must be covalently bound to the MUC1-targeting antibody. Such covalent conjugation requires the identification of a suitable conjugating reagent that will not impair the cytotoxic activity of PE38 and will not damage the immunoreactivity of the DMB5F3 mAb. Furthermore, the conjugation procedure itself will have to be optimized. These investigations although feasible are not trivial (see [38]) and are beyond the scope of the present study.

Improved conjugation techniques and the availability of stable linkers have accelerated the development of a number of targeted anti-tumor immunoconjugates [38–42]. Of particular interest, the recent approval of moxetumomab pasudotox-tdfk, an anti-CD22 cytotoxin for the treatment of relapsed hairy cell leukemia represents the first clinically applicable immunotoxin [39]. Because PE38 is the cytotoxin used in the moxetumomab ADC, its approval for clinical use is particularly relevant to the present study since PE38 exotoxin was used to generate the anti-MUC1-SEA DMB5F3 immunocomplex shown here to mediate potent in vivo anti-$MUC1^+$ tumor activity. In each of these ADCs or immunotoxin, the target antigen is not tumor-specific. Rather, the ADC targets molecules normally expressed on both malignant and non-malignant cells, engendering toxicity by ADC cross-over binding [40]. Strategies have been devised to widen the therapeutic window of conjugates by limiting their deposition at sites other than the devised target [41, 43], and site-specific conjugation has been used to improve the pharmacokinetics of conjugates by lowering toxicity and increasing the therapeutic index [42].

The present study shows that the anti-MUC1 SEA-mediated DMB5F3 immunocomplex can serve both in the delivery and internalization of linked toxin, resulting in a marked in vivo reduction in MUC1$^+$ pancreatic cancer, an aggressive malignancy which once metastatic has proved to date to be all but unresponsive to therapy [44]. It should be stressed that the clinically approved ADCs cited above target cell-surface proteins expressed by both tumor and normal cells. This attribute is shared by the anti-MUC1-SEA ADC. Yet the quantitative and qualitative differences in MUC1 expression between normal and malignant cells are, as noted, likely to translate into limiting the toxicity of anti-MUC1 SEA-mediated ADC. Furthermore, the high-affinity binding of DMB5F3 lends itself to strategies for widening the anti-MUC1 SEA therapeutic window [40]. The DMB5F3 antibody binds a single antigenic site on the SEA moiety of the MUC1 molecule, in contrast to anti-VNTR antibodies which bind to a polymorphic array of 20–125 tandem repeats in the MUC1 α-chain, which is shed into the peripheral circulation (Fig. 1, Panel I). The anti-MUC1 SEA antibody binds to the cell-bound MUC1-SEA module and shows strong circumferential staining with MUC1$^+$ malignant pancreatic cells. These characteristics of MUC1 expression, together with the vigorous in vivo anti-tumor effect of the DMB5F3- immunocomplex, bode well for the development of effective anti-MUC1 SEA ADCs against high-mortality MUC1$^+$ tumors.

Conclusions

mAbs of the DMB series that all target the anti-MUC1-SEA domain, and each of which binds to MUC1-expressing cells, were sequenced. This revealed that the seven anti-MUC1-SEA domain mAbs cluster into four unique groups, and all sequences are presented here. In vivo analyses in the SCID mouse model of an Antibody Drug Conjugate (ADC) formed by non-covalent linkage of Pseudomonas exotoxin to the chimeric DMB5F3 (chDMB5F3) antibody showed a significant decrease in the growth of a human pancreatic tumor xenotransplant. These studies indicate that anti-MUC1-SEA domain mAbs target tumors in vivo and may be of therapeutic use in the clinical setting for MUC1 + ve tumors.

Author contributions EP, MC, IB, RGK, RZ, NIS, GH, CG, AB, AM, TG, DBR, and DHW contributed to the study conception and design. Material preparation, data collection, and analysis were performed by authors DHW, EP, MC, DBR, MC, AM, CG, AB, and NIS. The first draft of the manuscript was written by DHW, DBR and EP. EP, MC, IB, NIS, DBR, and DHW commented on the various versions of the manuscript and contributed to the actual writing and preparation of its final version. EP, MC, IB, RGK, RZ, NIS, GH, CG, AB, AM, TG, DBR, and DHW read and approved the final manuscript.

Funding Funded by Israel Cancer Association (Project 20112024) and Israel Science Foundation (Project 1167/10).

Compliance with ethical standards

Conflict of interest Daniel H. Wreschner and Daniel B. Rubinstein have ownership interest in BioModifying, LLC. All other authors declare that they have no conflict of interest.

Ethical Approval *Animal care and use* Use of mice was done under supervision of the Tel Aviv University Institutional Animal Care and Use Committee (TAU-IACUC), Study Approval License number L-04-12-003. To ameliorate suffering including methods of killing, animal welfare and steps were all performed in accordance with regulations stipulated by TAU-IACUC. *Samples used for immunohistochemical stainings* These were procured from the Biomax tissue bank, see http://biomax.us. With all required approvals therein. *Cell line authentication* Short Tandem Repeat (STR) analysis (PowerPlexW 1.2 System, Promega, Fitchburg, WI), as described [45], was used to validate the human cell lines. STR profiles were matched with the German Collection of Microorganisms and Cell Cultures (DSMZ) database. Cell lines were obtained as gifts from Prof. I. Keydar.

References

1. Nath S, Mukherjee P (2014) MUC1: a multifaceted oncoprotein with a key role in cancer progression. Trends Mol Med 20:332–342
2. Deng J, Wang L, Chen H, Li L, Ma Y, Ni J, Li Y (2013) The role of tumour-associated MUC1 in epithelial ovarian cancer metastasis and progression. Cancer Metastasis Rev 32:535–551
3. Rahn JJ, Dabbagh L, Pasdar M, Hugh JC (2001) The importance of MUC1 cellular localization in patients with breast carcinoma: an immunohistologic study of 71 patients and review of the literature. Cancer 91:1973–1982
4. Remmers N, Anderson JM, Linde EM, DiMaio DJ, Lazenby AJ, Wandall HH, Mandel U, Clausen H, Yu F, Hollingsworth MA (2013) Aberrant expression of mucin core proteins and o-linked glycans associated with progression of pancreatic cancer. Clin Cancer Res 19:1981–1993
5. Krishn SR, Kaur S, Smith LM, Johansson SL, Jain M, Patel A, Gautam SK, Hollingsworth MA, Mandel U, Clausen H, Lo WC, Fan WT, Manne U, Batra SK (2016) Mucins and associated glycan signatures in colon adenoma-carcinoma sequence: prospective pathological implication(s) for early diagnosis of colon cancer. Cancer Lett 374:304–314
6. Xu F, Liu F, Zhao H, An G, Feng G (2015) Prognostic significance of mucin antigen MUC1 in various human epithelial cancers: a meta-analysis. Medicine (Baltimore) 94:e2286
7. Cloosen S, Gratama J, van Leeuwen EB, Senden-Gijsbers BL, Oving EB, von Mensdorff-Pouilly S, Tarp MA, Mandel U, Clausen H, Germeraad WT, Bos GM (2006) Cancer specific Mucin-1 glycoforms are expressed on multiple myeloma. Br J Haematol 135:513–516
8. Guillaume T, Dehame V, Chevallier P, Peterlin P, Garnier A, Gregoire M, Pichinuk E, Rubinstein DB, Wreschner DH (2019) Targeting cell-bound MUC1 on myelomonocytic, monocytic leukemias and phenotypically defined leukemic stem cells with anti-SEA module antibodies. Exp Hematol 70:97–108
9. Rivalland G, Loveland B, Mitchell P (2015) Update on Mucin-1 immunotherapy in cancer: a clinical perspective. Exp Opin Biol Ther 15:1773–1787

10. Gendler SJ, Lancaster CA, Taylor-Papadimitriou J, Duhig T, Peat N, Burchell J, Pemberton L, Lalani EN, Wilson D (1990) Molecular cloning and expression of human tumor-associated polymorphic epithelial mucin. J Biol Chem 265:15286–15293
11. Ligtenberg MJ, Vos HL, Gennissen AM, Hilkens J (1990) Episialin, a carcinoma-associated mucin, is generated by a polymorphic gene encoding splice variants with alternative amino termini. J Biol Chem 265:5573–5578
12. Levitin F, Stern O, Weiss M, Gil-Henn C, Ziv R, Prokocimer Z, Smorodinsky NI, Rubinstein DB, Wreschner DH (2005) The MUC1 SEA module is a self-cleaving domain. J Biol Chem 280:33374–33386
13. Zrihan-Licht S, Baruch A, Elroy-Stein O, Keydar I, Wreschner DH (1994) Tyrosine phosphorylation of the MUC1 breast cancer membrane proteins. Cytokine receptor-like molecules. FEBS Lett 356:130–136
14. Wreschner DH, Hareuveni M, Tsarfaty I, Smorodinsky N, Horev J, Zaretsky J, Kotkes P, Weiss M, Lathe R, Dion A et al (1990) Human epithelial tumor antigen cDNA sequences. Differential splicing may generate multiple protein forms. Eur J Biochem 189:463–473
15. Macao B, Johansson DG, Hansson GC, Hard T (2006) Autoproteolysis coupled to protein folding in the SEA domain of the membrane-bound MUC1 mucin. Nat Struct Mol Biol 13:71–76
16. Fiedler W, DeDosso S, Cresta S, Weidmann J, Tessari A, Salzberg M, Dietrich B, Baumeister H, Goletz S, Gianni L, Sessa C (2016) A phase I study of PankoMab-GEX, a humanised glyco-optimised monoclonal antibody to a novel tumour-specific MUC1 glycopeptide epitope in patients with advanced carcinomas. Eur J Cancer 63:55–63
17. Ryuko K, Schol DJ, Snijdewint FG, von Mensdorff-Pouilly S, Poort-Keesom RJ, Karuntu-Wanamarta YA, Verstraeten RA, Miyazaki K, Kenemans P, Hilgers J (2000) Characterization of a new MUC1 monoclonal antibody (VU-2-G7) directed to the glycosylated PDTR sequence of MUC1. Tumour Biol 21:197–210
18. Zhou D, Xu L, Huang W, Tonn T (2018) Epitopes of MUC1 tandem repeats in cancer as revealed by antibody crystallography: toward glycopeptide signature-guided therapy. Molecules 23:1326
19. Kimura T, Finn OJ (2013) MUC1 immunotherapy is here to stay. Exp Opin Biol Ther 13:35–49
20. Ibrahim NK, Yariz KO, Bondarenko I, Manikhas A, Semiglazov V, Alyasova A, Komisarenko V, Shparyk Y, Murray JL, Jones D, Senderovich S, Chau A, Erlandsson F, Acton G, Pegram M (2011) Randomized phase II trial of letrozole plus anti-MUC1 antibody AS1402 in hormone receptor-positive locally advanced or metastatic breast cancer. Clin Cancer Res 17:6822–6830
21. Rubinstein DB, Karmely M, Ziv R, Benhar I, Leitner O, Baron S, Katz BZ, Wreschner DH (2006) MUC1/X protein immunization enhances cDNA immunization in generating anti-MUC1 alpha/beta junction antibodies that target malignant cells. Cancer Res 66:11247–11253
22. Pichinuk E, Benhar I, Jacobi O, Chalik M, Weiss L, Ziv R, Sympson C, Karwa A, Smorodinsky NI, Rubinstein DB, Wreschner DH (2012) Antibody targeting of cell-bound MUC1 SEA domain kills tumor cells. Cancer Res 72:3324–3336
23. Rubinstein DB, Karmely M, Pichinuk E, Ziv R, Benhar I, Feng N, Smorodinsky NI, Wreschner DH (2009) The MUC1 oncoprotein as a functional target: immunotoxin binding to alpha/beta junction mediates cell killing. Int J Cancer 124:46–54
24. Mazor Y, Barnea I, Keydar I, Benhar I (2007) Antibody internalization studied using a novel IgG binding toxin fusion. J Immunol Methods 321:41–59
25. Tomayko MM, Reynolds CP (1989) Determination of subcutaneous tumor size in athymic (nude) mice. Cancer Chemother Pharmacol 24:148–154
26. Chalick M, Jacobi O, Pichinuk E, Garbar C, Bensussan A, Meeker A, Ziv R, Zehavi T, Smorodinsky NI, Hilkens J, Hanisch FG, Rubinstein DB, Wreschner DH (2016) MUC1-ARF-A novel MUC1 protein that resides in the nucleus and is expressed by alternate reading frame translation of MUC1 mRNA. PLoS ONE 11:e0165031
27. Gold DV, Karanjawala Z, Modrak DE, Goldenberg DM, Hruban RH (2007) PAM4-reactive MUC1 is a biomarker for early pancreatic adenocarcinoma. Clin Cancer Res 13:7380–7387
28. Sharkey RM, Goldenberg DM (2006) Targeted therapy of cancer: new prospects for antibodies and immunoconjugates. CA Cancer J Clin 56:226–243
29. Guo R, Guo W, Cao L, Liu H, Liu J, Xu H, Huang W, Wang F, Hong Z (2016) Fusion of an albumin-binding domain extends the half-life of immunotoxins. Int J Pharm 511:538–549
30. Tarp MA, Sorensen AL, Mandel U, Paulsen H, Burchell J, Taylor-Papadimitriou J, Clausen H (2007) Identification of a novel cancer-specific immunodominant glycopeptide epitope in the MUC1 tandem repeat. Glycobiology 17:197–209
31. Panchamoorthy G, Jin C, Raina D, Bharti A, Yamamoto M, Adeebge D, Zhao Q, Bronson R, Jiang S, Li L, Suzuki Y, Tagde A, Ghoroghchian PP, Wong KK, Kharbanda S, Kufe D (2018) Targeting the human MUC1-C oncoprotein with an antibody-drug conjugate. JCI Insight. https://doi.org/10.1172/jci.insight.99880
32. Scott AM, Allison JP, Wolchok JD (2012) Monoclonal antibodies in cancer therapy. Cancer Immun 12:14
33. Finn OJ (2017) Human tumor antigens yesterday, today, and tomorrow, cancer. Immunol Res 5:347–354
34. Horm TM, Schroeder JA (2013) MUC1 and metastatic cancer: expression, function and therapeutic targeting. Cell Adhes Migr 7:187–198
35. Wong N, Major P, Kapoor A, Wei F, Yan J, Aziz T, Zheng M, Jayasekera D, Cutz JC, Chow MJ, Tang D (2016) Amplification of MUC1 in prostate cancer metastasis and CRPC development. Oncotarget 7:83115–83133
36. Jarantow SW, Bushey BS, Pardinas JR, Boakye K, Lacy ER, Sanders R, Sepulveda MA, Moores SL, Chiu ML (2015) Impact of cell-surface antigen expression on target engagement and function of an epidermal growth factor receptor x c-MET bispecific antibody. J Biol Chem 290:24689–24704
37. Peat N, Gendler SJ, Lalani N, Duhig T, Taylor-Papadimitriou J (1992) Tissue-specific expression of a human polymorphic epithelial mucin (MUC1) in transgenic mice. Cancer Res 52:1954–1960
38. Xu H, Gan L, Han Y, Da Y, Xiong J, Hong S, Zhao Q, Song N, Cai X, Jiang X (2019) Site-specific labeling of an anti-MUC1 antibody: probing the effects of conjugation and linker chemistry on the internalization process. RSC Adv 9:1909–1917
39. Janus A, Robak T (2019) Moxetumomab pasudotox for the treatment of hairy cell leukemia. Exp Opin Biol Ther 19:501–508
40. de Goeij BE, Lambert JM (2016) New developments for antibody-drug conjugate-based therapeutic approaches. Curr Opin Immunol 40:14–23
41. Advani A, Coiffier B, Czuczman MS, Dreyling M, Foran J, Gine E, Gisselbrecht C, Ketterer N, Nasta S, Rohatiner A, Schmidt-Wolf IG, Schuler M, Sierra J, Smith MR, Verhoef G, Winter JN, Boni J, Vandendries E, Shapiro M, Fayad L (2010) Safety, pharmacokinetics, and preliminary clinical activity of inotuzumab ozogamicin, a novel immunoconjugate for the treatment of B-cell non-Hodgkin's lymphoma: results of a phase I study. J Clin Oncol 28:2085–2093
42. Strop P, Delaria K, Foletti D, Witt JM, Hasa-Moreno A, Poulsen K, Casas MG, Dorywalska M, Farias S, Pios A, Lui V, Dushin R, Zhou D, Navaratnam T, Tran TT, Sutton J, Lindquist KC, Han B, Liu SH, Shelton DL, Pons J, Rajpal A (2015) Site-specific conjugation improves therapeutic index of antibody drug conjugates with high drug loading. Nat Biotechnol 33:694–696

43. Younes A, Bartlett NL, Leonard JP, Kennedy DA, Lynch CM, Sievers EL, Forero-Torres A (2010) Brentuximab vedotin (SGN-35) for relapsed CD30-positive lymphomas. N Engl J Med 363:1812–1821
44. Neoptolemos JP, Kleeff J, Michl P, Costello E, Greenhalf W, Palmer DH (2018) Therapeutic developments in pancreatic cancer: current and future perspectives. Nat Rev Gastroenterol Hepatol 15:333–348
45. Grigoriadis A, Mackay A, Noel E, Wu PJ, Natrajan R, Frankum J, Reis-Filho JS, Tutt A (2012) Molecular characterisation of cell line models for triple-negative breast cancers. BMC Genom 13:619